Slip knots and unfastening topologies enhance toughness without reducing strength of silk fibroin fibers

Alice Berardo[1], Maria F. Pantano[1], Nicola M. Pugno[1,2,3]*

[1]Laboratory of Bio-inspired & Graphene Nanomechanics, Department of Civil, Environmental and Mechanical Engineering, University of Trento, Via Mesiano 77, 38123 Trento, Italy
[2]Center for Materials and Microsystems, Fondazione Bruno Kessler, Via Sommarive 18, 38123 Povo (TN), Italy
[3]School of Engineering and Materials Science, Queen Mary University of London, Mile End Road, London E1 4NS, U.K.

*Corresponding author: nicola.pugno@unitn.it

Abstract. Combination of high strength and high toughness is a desirable feature that structural materials should display. However, while in the past engineers had to accept a compromise, thus preferring either stronger or tougher materials depending on the requested application, nowadays new toughening strategies are available to provide strong materials with high toughness, too. In the present paper, we focus on one of such strategies, which requires no chemical treatment, but the implementation of slip knots with optimized shape and size in the involved material, which is silkworm silk in this case. In particular, a variety of slip knot topologies with different unfastening mechanisms are investigated including even complex knots usually used in textile industry and their efficiency in enhancing toughness of silk fibers is discussed.

Keywords: Knots, biomaterials, toughness, fibers

1. INTRODUCTION

Availability of materials provided with both high strength and high toughness is greatly desirable in structural applications, although in the past engineers had to accept a compromise preferring one or the other property depending on the requested application. In fact, strong materials traditionally displayed poor deformation capability and thus low specific energy dissipation potential [1]. However, recent developments in materials science have released new techniques taking inspiration from nature, which has already overcome the conflict between strength and toughness providing materials, like nacre and bones, with complex structures cooperating at different length scales [2-4]. Then, such concept has been transferred to engineering materials, introducing for example weak interfaces with intricate architectures [5] or dispersing fibers in a brittle matrix to form a bridge complementing crack opening and fracture [6].

While all of these solutions require some chemical treatment to be performed on the material of interest, in the present paper we considered a different toughening strategy which operates at a micro length scale and allows to significantly increase toughness of as-produced fibers. This follows an idea recently proposed by one of the authors [7] and requires the introduction within a fiber of a sliding frictional element, e.g., a knot. In fact, when the opposite ends of a knotted fiber are pulled apart, a hidden length is revealed through a sliding mechanism which dissipates a huge amount of energy. Basically, such mechanism reproduces at a microscopic level the breakage of weak bonds (i.e., sacrificial bonds) in highly coiled macromolecules, which allow molecular backbone to be further stretched with beneficial effects on toughness [8].

The fibers considered in the present study have natural origin, as they are extracted from silkworm silk cocoons. In fact, because of its unique combination of biocompatibility, physical and mechanical properties [9,10] silkworm silk is attracting increasing interest with a variety of biomedical applications, including tissue engineering scaffolds [11-12], drug delivery [13], sensors [14], as well as composites [15]. Such interest motivates also the need to further improve silk properties, like its energy dissipation capability (i.e., toughness) [16].

In the present paper, the toughness of single silk fibers was increased through the introduction of knots with optimized shape and size. In fact, different kinds of knots can be encountered in everyday life as well as in a variety of scientific fields with studies of mathematics [17], polymer science [18-19], colloids [20-21], fluids [22], chemistry [23-24] and biology [25-26] reporting application of knots. However, in this paper we investigated those topologies which allow to maximize the toughness increase without compromising the fiber strength. For this reason, as in our earlier work [27], our attention was focused on slip or running knots, which can be unfastened without inducing stress concentration and premature failure to the fiber. In the following, four topologies are considered, involving different unfastening mechanisms and design complexities, with some of them well known in textile industry with the aim of providing new and feasible tools for optimizing systems where energy dissipation is highly requested.

2. METHODS

2.1. Preparation of samples with different slip knot topologies

In the following sections, we report experiments carried out on single fibers extracted from *Bombyx mori* silkworm silk cocoons. In particular, before fibers extraction, as-produced cocoons underwent a standard degumming process [28], consisting of boiling twice with 1.1 g/L and 0.4 g/L Na_2CO_3 (anhydrous, minimum 99%, from Sigma Aldrich) water solution for one hour each time, washing against distilled water and air-drying. In this way, it was possible to obtain silk fibroin fibers released from their natural binding layer (i.e., sericin) which has no load bearing capacity [29].
Then, single fibroin fibers were manipulated by tweezers in order to design knots with proper topology. The knots implemented in our experiments were chosen in order to guarantee the fiber to be highly stressed within a sufficiently large strain interval when its opposite ends are pulled apart (as during a tensile test), but without introducing stress concentration, which could lead to premature failure. Under these conditions, in fact, the introduction of a knot is able to modify the stress-strain curve of the fibers, introducing an artificial plastic-like plateau with an even significant increase of their toughness [7].

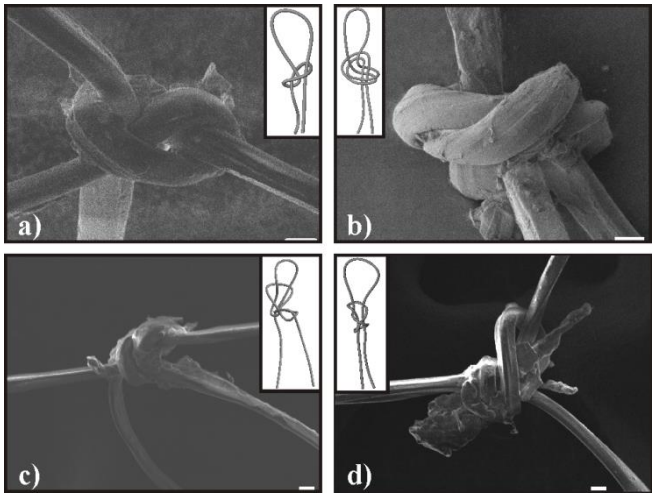

Figure 1: Gallery of knots implemented in single silk fibers. (a) SEM picture of the *Noose* with a schematic on top. (b) SEM picture of the *Overhand Loop* with a schematic on top. (c) SEM picture of the *Chain Knot* with two chains and a schematic on top. (d) SEM picture of the *X-Knot* with a schematic on top. Scale bar: 10 μm.

In order for the knot to not affect the fiber strength, it is necessary that it can be completely released as the fiber ends are pulled apart. Thus, only slip knots were herein considered. In our earlier work

[27] we implemented two different slip knot topologies in single silk fibers, which are known as *Noose* and *Overhand Loop* [30] (Figure 1a-b). While the *Noose* requires the fiber to be turned once around itself, the *Overhand Loop* requires the fiber to be first folded and then turned around itself, thus involving a different unfastening mechanism. In fact, in the first case the knot tends to untie as the fiber ends are pulled apart. Thus, at the beginning this can be very tight causing the fiber to be highly stressed during the whole tensile test and its toughness to be significantly increased. On the contrary, in the *Overhand Loop* the knot tends to further tie, requiring to start from a very loose configuration in order to be completely released, with much less toughness enhancement. As a consequence, in the present work we investigated and optimized other slip knot topologies which are strictly related to the *Noose* in order to explore the possibility to further improve our previous results.

The first topology we considered is an open version of the *Monkey Chain Lanyard Knot* [30], which is well known in textile industry, as this reproduces a chain stitch of crochet (Figure 1c): after a noose is tightened, one thread of the fiber is folded and forced to cross the loop, which ends in a chain of a chain stitch. In some samples, such steps were repeated in order to build chain stitch with four and six chains, respectively. In the following, for the sake of brevity, such knot topology will be referred to as simply *Chain Knot*.

The second topology (Figure 1d), which has no common name, requires first the implementation of a noose [30]; then, its loop is turned inside the knot, obtaining an x-shaped knot, which is for this reason referred to as *X-Knot* topology in the following.

All the produced samples were obtained from a fiber with initial length (l) equal to 20 mm, mounted on a paper frame in order for the fiber ends to be 10 mm apart (l_0) and with a length involved in the loop (l_p) of about 10 mm (Figure 2a-b).

2.2 Estimation of toughness increase due to knots

The energy per unit mass (i.e., toughness modulus, T_u) dissipated by an unknotted fiber during a tensile test is related to the area under its stress-strain curve (Figure 2a) as:

$$T_u = 1/m \int_0^{x_f} F dx = Al/m \int_0^{\varepsilon_f} \sigma d\varepsilon \ = 1/\rho \int_0^{\varepsilon_f} \sigma d\varepsilon \tag{1}$$

where m is the fiber mass, x_f is the displacement at fracture, F is the applied load, A is the fiber cross sectional area, l is the fiber initial length, ρ is the volumetric density, $\varepsilon_f = (l_f - l)/l = x_f/l$ is the fracture strain, l_f is the fiber final length, and $\int_0^{\varepsilon_f} \sigma d\varepsilon$ is the area under the stress-strain curve.

If a knot is introduced in a fiber (Figure 2b), expression (1) has to be modified in order to take into account the fiber length involved in both the knot (negligible) and the loop, with its toughness modulus, T_k, which can be computed as:

$$T_k = 1/m \int_0^{x_f^*} F dx = Al_0/m \int_0^{\varepsilon_f^*} \sigma d\varepsilon = (1 - k_1)/\rho \int_0^{\varepsilon_f^*} \sigma d\varepsilon \tag{2}$$

where $x_f^* = l - l_0 + x_f$, l_0 is the initial length equal to the distance between the fiber opposite ends, $\varepsilon_f^* = x_f^*/l_0$, $k_1 = (l - l_0)/l$ accounting for the difference between l_0 and l and $\int_0^{\varepsilon_f^*} \sigma d\varepsilon$ is the area under the stress-strain curve of the knotted fiber [7].

When the opposite ends of a knotted fiber are pulled apart, the knot presence causes alternating cycles of loading (the knot is tightened and the fiber is stressed) and unloading (the knot unties, some fiber length is released from the loop, causing stress relaxation) until the knot loosens completely (Figure 2b). In all our tests, the final part of the stress-strain curve of knotted fibers reproduced the stress-strain curve of the corresponding unknotted fibers, showing in fact a stress at break comparable with the strength of reference samples (without any knots and extracted from a cocoon region adjacent to the knotted fiber) tested apart (Figure 2a-b). Moreover, since it is well known that silk mechanical properties show significant variability [31], it is preferable to compare the toughness of a knotted fiber to the toughness of the same fiber in unknotted configuration. For this reason, we considered the final part of the stress-strain curve of a knotted fiber as the curve of its reference unknotted fiber. Then, the ratio between the toughness of the knotted fiber, T_k, and the toughness of the corresponding unknotted fiber, T_u', can be obtained with the following expression:

$$T_k/T_u' = \left[Al_0/m \int_0^{\varepsilon_f^*} \sigma d\varepsilon\right] \Big/ \left[Al_0/m \int_{\varepsilon^*}^{\varepsilon_f^*} \sigma d\varepsilon\right] = \int_0^{\varepsilon_f^*} \sigma d\varepsilon \Big/ \int_{\varepsilon^*}^{\varepsilon_f^*} \sigma d\varepsilon \quad (3)$$

where $\int_{\varepsilon^*}^{\varepsilon_f^*} \sigma d\varepsilon$ is the area under the final part of the stress-strain curve, where the knot is completely released.

However, in case it is not possible to consider the same fiber for comparison, since the final part of the stress-strain curve does not clearly show the behavior of the fiber in unknotted configuration, then we can estimate the toughness increase referring to the toughness modulus of an unknotted fiber extracted from a cocoon region adjacent to that of the knotted fiber in order to limit variations in physical and mechanical properties. In this way the area under the stress-strain curve of the knotted fiber has to be scaled by the factor $(1\text{-}k_1)$:

$$T_k/T_u = \left[(1-k_1)/\rho \int_0^{\varepsilon_f^*} \sigma d\varepsilon\right] \Big/ \left[1/\rho \int_0^{\varepsilon_f} \sigma d\varepsilon\right] = (1-k_1) \int_0^{\varepsilon_f^*} \sigma d\varepsilon \Big/ \int_0^{\varepsilon_f} \sigma d\varepsilon \ . \quad (4)$$

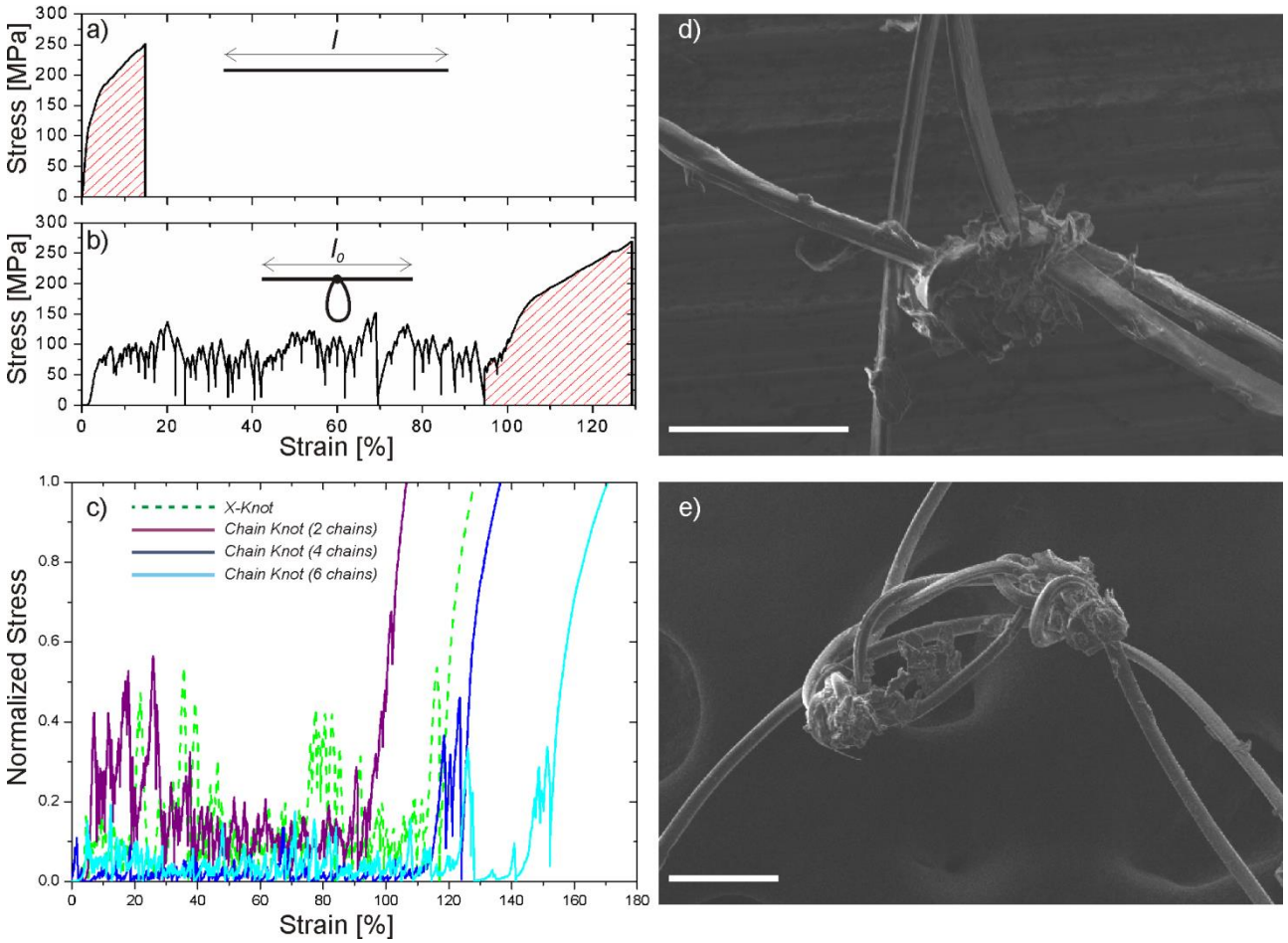

Figure 2: (a) Stress-strain curve of an unknotted natural fiber with length *l*. (b) Stress-strain curve of a knotted natural fiber with length *l* and distance between its opposite ends l_0, which was extracted from a cocoon region adjacent to the unknotted fiber (a). The presence of the knot modifies the shape of the stress-strain curve (a), introducing a plastic-like plateau and leaving a final region (highlighted) almost corresponding to the stress-strain curve of the same fiber with unknotted configuration. The strain interval within this final region appears larger than in (a) since it is computed with respect to l_0 instead of *l*. (c) Comparison between the stress-strain curves derived from samples with an *X-Knot* and a *Chain Knot* with either 2, 4 or 6 chains, respectively. Here, stress values are normalized with respect to the fracture stress of each fiber. (d) SEM image of a fiber with a *Chain Knot* with four chains visibly damaged by preparation, which caused superficial exfoliation. (e) SEM image of a fiber with a *Chain Knot* with six chains not uniformly tightened during preparation. Scale bar: 100 µm.

3. RESULTS

To evaluate the toughness enhancement due to knot introduction we performed tensile tests on more than 50 samples provided with a knot with either of the topologies described in the previous sections. Tests were carried out at room temperature at a strain rate of 0.002 s^{-1} by a nanotensile testing machine (Agilent T150 UTM). Following a common approach reported in the literature [29], stress was computed considering each fiber as provided with a circular cross section, which was evaluated through optical microscope and Scanning Electron Microscope (SEM). The average diameter of the fibres was 11.5 ± 1.5 µm. All knotted fibres broke at a stress level of about 420+130MPa, which matches the typical strength of pristine silk fibres. Figure 2c reports four stress-strain curves, one for each knot topology we tested. In all the cases, with respect to the stress strain curve of a sample with no knots (Figure 2a), there is a series of loading and unloading events

caused by fiber sliding into its loop through the knot and related stick-slips, as explained in the previous section. Furthermore, it is interesting to observe that at the end of the test, before the knot loosens completely and the curve collapses into the stress-strain curve of an unknotted fiber, there are some pronounced stress peaks, which correspond to the number of times the fiber was turned around itself during preparation. In fact, the number of final stress peaks, which are the main responsible for toughness increase, is more visible in case of a chain knot with four and six chains.

Table 1. Comparison (*) between the toughness increases and strength decreases provided by different knot topologies with respect to unknotted single silk fibers (average strength of 514 ± 103 MPa and average toughness modulus: 32 ± 14 J/g computed considering a density of 1.4 g/cm^3 [32]).

KNOT TOPOLOGY	NUMBER OF TESTS	TOUGHNESS INCREASE (%)	STRENGTH DECREASE (%)
Noose	14	284 ± 43	32 ± 29
Overhand Loop	20	118 ± 19	21 ± 37
X-Knot	8	450 ± 107	18 ± 27
Chain Knot with 2 chains	11	310 ± 11	7 ± 35
Chain Knot with 4 chains	6	150 ± 11	19 ± 27
Chain Knot with 6 chains	5	142 ± 18	11 ± 30

(*) Because of variability in the knot tightening procedure, the knot size shows some difference from sample to sample. Thus, when we computed the toughness enhancement provided by each knot topology, we considered an average over three results representative of their optimized behavior.

As evolution of the *Noose*, all knot topologies could be firmly tightened and then completely unfastened during the test with quite high energy dissipation (Table 1), depending on the stress plateau value introduced in the corresponding stress-strain curve (Figure 2c). In particular, samples with a chain knot with two chains showed a stress-strain curve with a well-defined plastic-like plateau between one eighth and a quarter of the fracture strength (Figure 2c), providing a toughness increase of about 300%, which is comparable to the result obtained with the *Noose* [27]. When the number of chains is increased, there is no evident trend in toughness enhancement (Table 1). In fact, even if some samples with a chain knot with four chains provided some significant toughness enhancement of almost 400%, the average value is much lower, being about 150%, which is comparable to the average result provided by chain knots with six chains. However, such values are still bigger than the one recorded for the *Overhand Loop* (Table 1).
On the contrary, *X-Knot* topology, providing a higher plateau in samples stress-strain curve, with average values of about one fifth of the fracture stress (Figure 2c) resulted in a toughness enhancement up to 450% on average (Table 1).

4. DISCUSSION

In order to understand the differences in toughness enhancement provided by the investigated knot topologies (Table 1), it is necessary to consider their own preparation procedure and unfastening mechanism (Figure 3). As we reported in [27], also in this case the lowest toughness enhancement was provided by the *Overhand loop*. In fact, this is the only topology where the knot tends to

further tie as the opposite ends of its hosting fiber are pulled apart. As a consequence, this is able to completely unfasten only when its initial configuration is considerably loose, thus causing small friction against fiber sliding and consequent limited toughness increase. On the contrary, the *Noose* can be very tight in its initial configuration, providing a high and wide plateau in the fiber stress-strain curve, which causes the toughness enhancement to be much higher (Table 1).

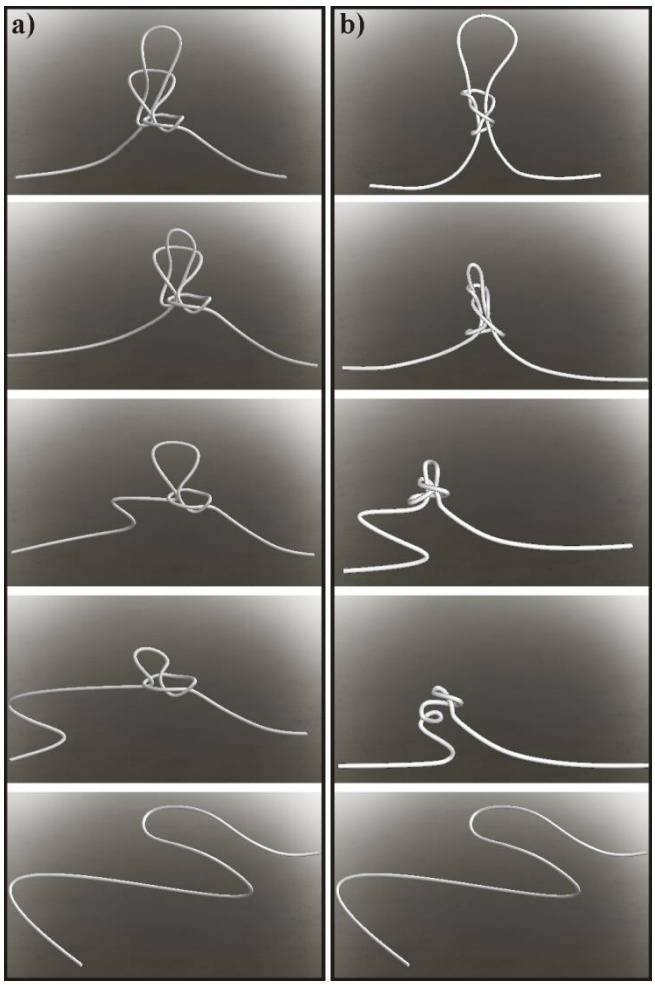

Figure 3: Untightening mechanism of the (a) *Chain Knot* (in this schematic with two chains) and (b) *X-Knot*. (a) When the fiber opposite ends are pulled apart, the loop is sucked into its closest chain until this is completely released, thus forcing the knot to collapse into a simple noose. If the fiber ends are pulled further apart, the noose loosens until the knot is completely untightened. (b) In an *X-knot*, the fiber appears to be turned twice at the bottom of its loop. When its opposite ends are pulled apart, the turn closer to the loop tends to tie, causing friction against the fiber sliding, while the other one loosens. In this way, the knot is always able to completely unfasten but a significant amount of energy can be dissipated.

Although the other knots considered in this work, the *Chain Knot* and *X-Knot*, evolve both from the *Noose*, they provided different results, which depend on a different sliding mechanism which the fiber experiences before the knot is completely unfastened (Figure 3). In this context, the *Chain Knot* behaves more similar to the *Noose*, since the chain which is closer to the loop tends to open as the fiber ends are pulled apart, thus the fiber can slide easily within the loop and the knot tends to further untie (Figure 3). On the contrary, a part of the *X-Knot* tends to tie when the fiber is pulled (Figure 3). In fact, the fiber appears to be turned twice, but while one turn (which is the closest to the loop) tends to tie as the fiber ends are pulled apart, the second one (on the opposite side) tends

to untie. This means that the knot can always be released, but with significant energy dissipation, causing the fiber to be much more stressed during the test and toughness to be more than four times bigger than the reference (Table 1).

We investigated also the influence of the number of chains on the friction potential of the *Chain Knot*. First of all, compared to other knots, chain knots with multiple chains require increasing manipulation, which on turn could induce some superficial exfoliations into the knotted fiber (Figure 2d). On one side, this could contribute in enhancing energy dissipated by friction during unfastening, as the fiber surface becomes rougher, but on the other side it could also affect the fiber fracture strength, if too damage is introduced. From a quantitative point of view, our results showed that the introduction of 2 chains in the chain knot provided about a twofold toughness increase with respect to the average data obtained with 4 and 6 chains, which were comparable (Table 1). This indicates that in the latter cases, the friction potential was not fully exploited, as it was difficult to guarantee all chains in the knot to be uniformly tightened (Figure 2e). Nevertheless, in some cases we achieved a much more significant increase of almost 400%, meaning that there is still room for further increasing, which could be achieved through implementation of a controlled and repeatable production process, as that used in textile industry, where such knot finds already common application.

5. CONCLUSIONS

In the present paper, we compared the effectiveness of different knot topologies in enhancing the toughness of single silk fibers. The knots considered herein were characterized by different design complexity, but had all the common feature to be able to completely unfasten when the fiber opposite ends were pulled apart. Such condition on one side allowed to not induce any stress concentration, which could cause premature failure of the fiber, and on the other side allowed to dissipate an even significant amount of energy depending on the knot design. Such results are very promising, since some of the tested knots are already known in textile industry. Thus, the availability of industrial machinery able to process knots with high quality and repeatability could easily allow them to be implemented in industrial products which require strong energy dissipation capability.

COMPETING INTERESTS

We have no competing interests.

ACKNOWLEDGEMENTS

The authors wish to thank Nello Serra from “Comunità don Milani” (Acri, CS, Italy) for kindly supplying the silk cocoons used in the experiments.

NMP is supported by the European Research Council (ERC StG Ideas 2011 BIHSNAM n. 279985 on “Bio-Inspired hierarchical super-nanomaterials”, ERC PoC 2015 SILKENE no. 693670 on “Bionic silk with graphene or other nanomaterials spun by silkworms”, ERC PoC 2013-2 KNOTOUGH n. 632277 on “Super-tough knotted fibres”), by the European Commission under the Graphene Flagship (WP10 "Nanocomposites", n. 604391) and by the Provincia Autonoma di Trento ("Graphene Nanocomposites", n. S116/2012-242637 and reg.delib. n. 2266).

REFERENCES

[1] Ritchie RO. 2011, The conflicts between strength and toughness, Nature Mat. 10: 817-822.

[2] Bouville F, Maire E, Meille S., Van de Moortèle B, Stevenson AJ, Deville S. 2014, Strong, tough and stiff bioinspired ceramics from brittle constituents, Nature Mat. 13: 508-514.
[3] Munch E, Launey ME, Alsem DH, Saiz E, Tomsia AP, Ritchie RO. 2008, Tough, Bio-Inspired Hybrid Materials, Science 5907: 1516-1520.
[4] Cranford SW, Tarakanova A, Pugno N, Buehler MJ. 2012, Nonlinear material behaviour of spider silk yields robust webs, Nature, 482, 72-78
[5] Mirkhalaf M, Khayer Dastjerdi A, Barthelat F. 2013, Overcoming the brittleness of glass through bio-inspiration and micro-architecture, Nature Comm 5:3166.
[6] Palmeri MJ, Putz KW and Brinson LC. 2010, Sacrificial Bonds in Stacked-Cup Carbon Nanofibers: Biomimetic Toughening Mechanisms for Composite Systems, ACS Nano 4 (7): 4256-4264.
[7] Pugno NM. 2014, The ‘‘Egg of Columbus’’ for Making the World’s Toughest Fibres. PlosOne; 9:, 4, e93079. (2014)
[8 Fantner GE, Oroudjev E, Schitter G, Golde LS, Thurner P, Finch MM, Turner P, Gutsmann T, Morse DE, Hansma H, Hansma PK. 2006, Sacrificial Bonds and Hidden Length: Unraveling Molecular Mesostructures in Tough Materials, Biophysical Journal 90: 1411–1418.
[9] Perez-Rigueiro, J, Viney, C, Llorca, J & Elices MJ. 1998, Silkworm Silk as an Engineering Material. J. Appl Polym Sci 70, 2439-2447.
[10] Altman HG, Diaz F, Jakuba C. Calabro T, Horan RL, Chen J, Lu H, Richmond J and Kaplan DL. 2003, Silk-based biomaterials. Biomaterials 24, 401-416.
[11] Ude AU, Ariffin AK and Azhari CH. 2013, An Experimental Investigation on the Response of Woven Natural Silk Fiber/Epoxy Sandwich Composite Panels Under Low Velocity Impact. Fiber Polym 14 (1), 127-132.
[12] Yodmuang S, McNamara SL, Nover AB, Mandal BB, Aganwal M, Kelly TAN, Chao PHG, Hung C , Kaplan DL,Vunjak-Novakovic G. 2015, Silk microfiber-reinforced silk hydrogel composites for functional cartilage tissue repair, Acta Biomater 11: 27-36.
[13] Meinel AJ, Kubowb KE, Klotzsch E, Garcia-Fuentes M, Smith ML, Vogel V, Merkle HP and Meinel L. 2009, Optimization strategies for electrospun silk fibroin tissue engineering scaffolds. Biomaterials, 30, 3058-3067.
[14] Tsioris K, Tilburey GE; Murphy AR, Domachuk P, Kaplan DL, Omenetto FG. 2010, Functionalized-Silk-Based Active Optofluidic Devices, Advanced Funcional Materials 20 (7): 1083-1089.
[15] Hardy JG, Romer LM and Scheibel T.R. 2008, Polymeric materials based on silk proteins. Polymer 49, 4309-4327.
[16] Shao Z and Vollrath F. 2002, Surprising strength of silkworm silk. Nature 418, 741.
[17] Anstee RP, Przytycki JH and Rolfsen D. 1989, Knot Polynomials and Generalized Mutation. Topol Appl 32, 237-249.
[18] Bayer RK. 1994, Structure transfer from a polymeric melt to the solid state-Part III: Influence of knots on structure and mechanical properties of semicrystalline polymers. Colloid Polym Sci 272, 910-932.
[19] Saitta AM, Soper PD, Wasserman E and Klein ML. 1999, Influence of a knot on the strength of a polymer strand. Nature 399, 46-48.
[20] Tkalec U, Ravnik M, Copar S, Zumer S, Musevic I. 2011, Reconfigurable Knots and Links in Chiral Nematic Colloids. Science; 333: 62.
[21] Sennyuk B, Liu Q, He S, Kamien RD, Kusner RB, Lubensky TC, Smalyukh I. 2013, Topological colloids. Nature; 493: 200-205.
[22] Kleckner D, Irvine WTM. 2013, Creation and dynamics of knotted vortices. Nat. Phys.; 9: 253-258.
[23] Forgan RS, Sauvage JP, Stoddart JF. 2011, Chemical Topology: Complex Molecular Knots, Links and Entanglements. Chem Rev; 111: 5434-5464.
[24] Ayme JF, Beves JE, Leigh DA, McBurney RT, Rissanen K, Schultz D. 2012, A synthetic molecular pentafoil knot. Nat Chem; 4: 15-20.

[25] Dean F, Stasiak A, Koller T, Cozzarelli N. 1985, Duplex DNA knots produced by Escherichia coli topoisomerase I. Structure and requirements for formation. J Biol Chem; 260: 4975-4983.
[26] He C, Lamour G, Xiao A, Gsponer J, Li H. 2014, Mechanically Tightening a Protein Slipknot into a Trefoil Knot. J Am Soc Chem; DOI: dx.doi.org/10.1021/ja503997h.
[27] Pantano MF, Berardo A, Pugno N. 2015 Tightening slip knots in raw and degummed silk to increase toughness without losing strength. Sci. Rep. 5, 18222.
[28] Bonani W, Maniglio D, Motta A, Tan W, Migliaresi C. 2011, Biohybrid nanofiber constructs with anisotropic biomechanical properties. J Biomed Mater Res B; 96B (2): 276-286.
[29] Perez-Rigueiro J, Viney C, Llorca J, Elices M. 2000, Mechanical properties of single-brin silkworm silk. J Appl Polym Sci; 75.1270-1277.
[30] Ashley CW. 1944, The Ashley book of knots. New York, NY: Doubleday, Doran and Co. Inc.
[31] Zhao HP, Feng XQ, Shi HJ. 2007, Variability in mechanical properties of Bombyx mori silk. Mater Sci Eng C; 27: 675-683.
[32] Ashby MF. 2011 Materials selection in mechanical design. Burlington, MA: Butterworth-Heinemann.